43. P. A. Martin, D. W. Lea, T. A. Mashiotta, T. Papenfuss, M. Sarnthein, *Geochem. Geophys. Geosyst.* [online] **1**, paper number 1999GC000006 (1999). Available at: http://g-cubed.org
44. D. T. Rodbell *et al.*, *Science* **283**, 516 (1999).
45. D. H. Sandweiss, J. B. Richardson III, E. J. Reitz, H. B. Rollins, K. A. Maasch, *Science* **273**, 1531 (1996).
46. J. Shulmeister, B. Lees, *Holocene* **5**, 10 (1995).
47. T. M. Rittenour, J. Brigham-Grette, M. E. Mann, *Science* **288**, 1039 (2000).
48. A. C. Clement, R. Seager, M. A. Cane, *Paleoceanography* **15**, 731 (2000).
49. Z. Liu, J. Kutzbach, L. Wu, *Geophys. Res. Lett.* **27**, 2265 (2000).
50. B. L. Otto-Bliesner, *Geophys. Res. Lett.* **26**, 87 (1999).
51. A. Berger, *J. Atmos. Sci.* **35**, 2362 (1978).
52. K. A. Hughen, D. P. Schrag, S. B. Jacobsen, *Geophys. Res. Lett.* **26**, 3129 (1999).
53. D. Paillard, L. Labeyrie, P. Yiou, *EOS* **77**, 379 (1996).
54. M. T. McCulloch *et al.*, *Science* **283**, 202 (1999).
55. T. Mitsuguchi, E. Matsumoto, O. Abe, T. Uchida, P. Isdale, *Science* **274**, 961 (1996).
56. G. T. Shen, R. B. Dunbar, *Geochim. Cosmochim. Acta* **59**, 2009 (1995).
57. D. P. Schrag, G. Hampt, D. W. Murray, *Science* **272**, 1930 (1996).
58. R. W. Reynolds, T. M. Smith, *J. Clim.* **7**, 929 (1994).
59. N. A. Rayner, E. B. Horton, D. E. Parker, C. K. Folland, R. B. Hackett, *Version 2.2 of the Global Sea-Ice and Sea Surface Temperature Data Set 1903–1994, Climate Research Technical Note 74* (Hadley Centre for Climate Prediction and Research, Bracknell, UK, 1996).
60. A. Kaplan *et al.*, *J. Geophys. Res.* **103 C9**, 18567 (1998).
61. N. J. Shackleton, *Science* **289**, 1897 (2000).
62. J. Chappell *et al.*, *Earth Planet. Sci. Lett.* **141**, 227 (1996).
63. J. Chappell, N. J. Shackleton, *Nature* **324**, 137 (1986).
64. T. M. Esat, M. T. McCulloch, J. Chappell, B. Pillans, A. Omura, *Science* **283**, 197 (1999).

65. We thank A. Clement for providing the data for Fig. 5D and for comments on an earlier draft of the manuscript, M. Cane and M. Mann for discussion on statistical analysis, and G. Mortimer for help in chemical procedures. Lamont-Doherty Publication no. 6140. Supported by UK Natural Environment Research Council grant GR3/09961.

1 December 2000; accepted 11 January 2001
Published online 25 January 2001;
10.1126/science.1057969
Include this information when citing this paper.

REPORTS

Observation of $d_{x^2-y^2}$–Like Superconducting Gap in an Electron-Doped High-Temperature Superconductor

T. Sato,[1] T. Kamiyama,[1] T. Takahashi,[1]* K. Kurahashi,[1] K. Yamada[2]

High-resolution angle-resolved photoemission spectroscopy of the electron-doped high-temperature superconductor $Nd_{2-x}Ce_xCuO_4$ (x = 0.15, transition temperature T_c = 22 K) has found the quasiparticle signature as well as the anisotropic $d_{x^2-y^2}$–like superconducting gap. The spectral line shape at the superconducting state shows a strong anisotropic nature of the many-body interaction. The result suggests that the electron-hole symmetry is present in the high-temperature superconductors.

The symmetry of the superconducting gap is directly related to the origin of superconductivity (*1*). For the hole-doped high-temperature superconductors (HTSCs), such as $La_{2-x}Sr_xCuO_4$ (LSCO), $YBa_2Cu_3O_7$ (YBCO), and $Bi_2Sr_2CaCu_2O_8$ (BSCCO), the general consensus is that they have an anisotropic $d_{x^2-y^2}$–like superconducting gap. But measurements from tunneling spectroscopy and magnetic penetration depth (*2–4*) experiments suggest that the electron-doped HTSCs such as $Pr_{2-x}Ce_xCuO_4$ (PCCO) and $Nd_{2-x}Ce_xCuO_4$ (NCCO) may have a different superconducting order parameter, possibly *s*-wave. The electron-doped HTSCs also appear different from their hole-doped counterparts in many physical properties such as displaying a narrower doping range of the superconducting phase (*5*). The relatively low maximum T_c (~25 K) and the electrical and thermal properties, interpreted by the Fermi liquid–like T^2 dependence, favor an *s*-wave symmetry. Thus, it has been believed that the superconducting order parameter and, therefore, the origin of superconductivity mechanism may be different for the hole- and the electron-doped HTSCs. However, recent tunneling (*6*), scanning SQUID (superconducting quantum interference device) microscope (*7*), and magnetic-penetration-depth (*8*, *9*) experiments have raised a question on this scenario, suggesting a *d*-wave symmetry for both types, whereas some other experiments (*10*, *11*) support the distinct difference in the superconducting order parameter between the two "different" HTSCs. Angle-resolved photoemission spectroscopy (ARPES) is powerful experimental technique to study the momentum-resolved (*k*-resolved) electronic structure of a material and has made an important contribution in establishing the superconducting order parameter in the hole-doped HTSCs (*12*, *13*). In comparison to the hole-doped HTSCs, the application of ARPES to study electron-doped HTSCs has not been so advanced. This has been due to the insufficient energy resolution to resolve the superconducting gap, which is much smaller than those of the hole-doped HTSCs, and due to the difficulty in growing high-quality single crystals of electron-doped samples.

We report high-resolution ARPES data on a high quality $Nd_{2-x}Ce_xCuO_4$ (x = 0.15, T_c = 22 K) single crystal and show that the NCCO has an anisotropic superconducting gap well described by the $d_{x^2-y^2}$-wave (*14*). The result suggests that electron-hole symmetry holds in the HTSCs and that the basic framework of the superconducting mechanism is similar between the electron- and the hole-doped HTSCs.

Single crystals of $Nd_{2-x}Ce_xCuO_4$ (x = 0.15, T_c = 22 K) were grown by the traveling-solvent floating-zone method and annealed in flowing Ar gas at 950°C for 10 hours. The magnetic susceptibility measurement shows that T_c is 22 K with a width of 2 K. ARPES measurements were performed using a SCIENTA SES-200 spectrometer with a high-flux discharge lamp and a toroidal grating monochromator. The energy and angular (momentum) resolutions were set at 12 meV (full width at half maximum) and ±0.1° (±0.01 $Å^{-1}$), respectively. A clean, flat surface of samples was obtained by in situ cleaving under ultrahigh vacuum of 5×10^{-11} Torr. Samples were cooled down by using a liquid He flow cryostat, and the temperature of the sample was monitored by a silicon diode thermocouple embedded in the sample substrate. Because surface degradation was found to occur relatively quickly, all spectra were recorded at 10 K within 2 hours after cleaving (*15*), during which any sign of degradation or contamination of the sample surface was not observed. We have confirmed the reproducibility of data with several different cleaves and samples. The Fermi level (E_F) of sample was referenced to that of a gold film evaporated onto the sample substrate.

The representative valence-band ARPES

[1]Department of Physics, Tohoku University, Sendai 980-8578, Japan. [2]Institute for Chemical Research, Kyoto University, Uji 611-0011, Japan.

*To whom correspondence should be addressed. E-mail: t.takahashi@msp.phys.tohoku.ac.jp

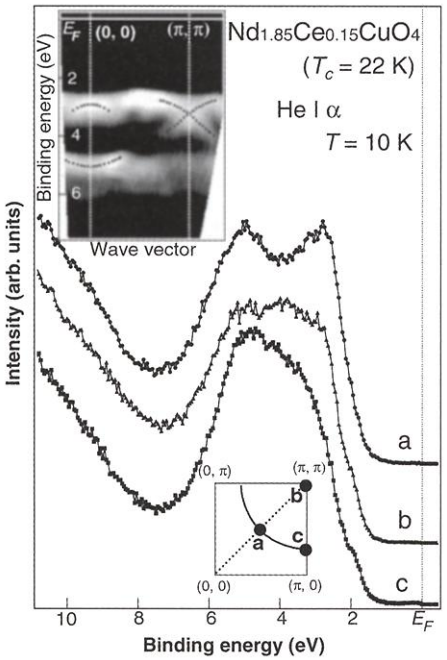

Fig. 1. Angle-resolved valence-band photoemission spectra of $Nd_{2-x}Ce_xCuO_4$ (x = 0.15, T_c = 22 K), measured at or near the high-symmetry points in the Brillouin zone with the He Iα line (21.218 eV) at 10 K. Inset shows the band dispersions along the (0,0)-(π,π) cut obtained by taking the second derivative of ARPES spectra.

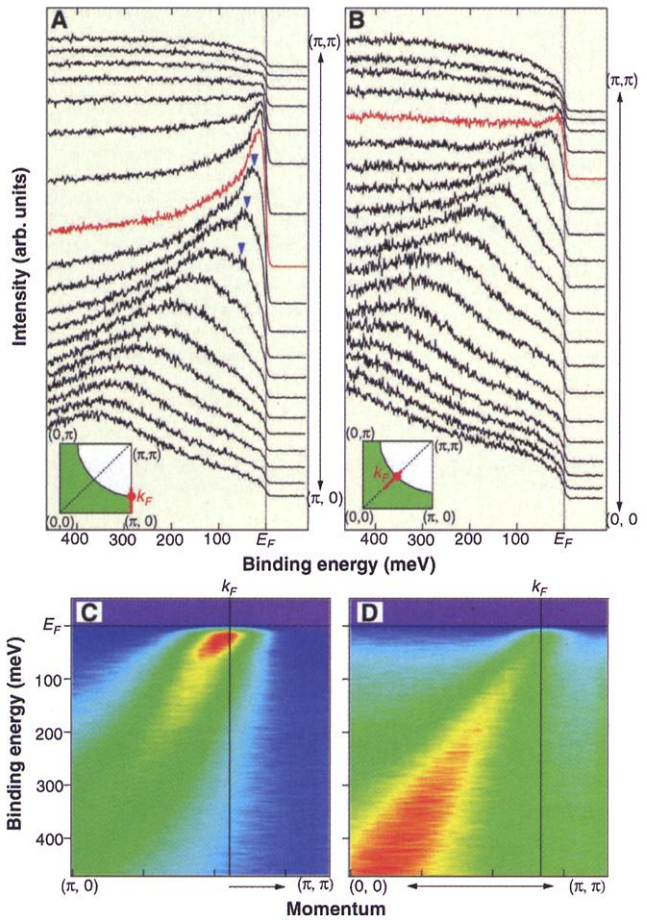

Fig. 2. Angle-resolved photoemission spectra of $Nd_{2-x}Ce_xCuO_4$ (x = 0.15, T_c = 22 K) measured at 10 K along the (**A**) (π,0)-(π,π) cut and (**B**) (0,0)-(π,π) cut. Spectra at the Fermi momentum (k_F) determined by the minimum-gap-locus method (*29*) are shown in red. The ARPES spectral intensity is plotted as a function of the binding energy and the momentum in (**C**) and (**D**) for the two directions, respectively.

spectra of $Nd_{2-x}Ce_xCuO_4$ (x = 0.15, T_c = 22 K), measured at or near the high-symmetry points in the Brillouin zone (Fig. 1), are consistent with previous ARPES reports (*16–18*). There is no "dirty peak" at 9-eV binding energy in the spectra, which is regarded as a fingerprint for a dirty or degraded surface. The inset shows the band dispersions along the (0,0)-(π,π) cut obtained by taking the second derivative of ARPES spectra. We find that the bands show a symmetric behavior with respect to the high-symmetry points in the bulk Brillouin zone, indicating that their nature is bulk in origin.

The ARPES spectra in the vicinity of E_F measured at 10 K along the two high-symmetry lines in the Brillouin zone are shown [Fig. 2: A, (π,0)-(π π) and B, (0,0)-(π,π)]. The intensity of ARPES spectra is plotted as a function of the binding energy and the momentum for the two directions (Fig. 2, C and D, respectively). We find that there is a strong dispersive feature approaching E_F in both directions, suggesting a hole-like Fermi surface centered at the (π,π) point as in BSCCO (*19*, *20*), consistent with the previous report (*21*). The energy dispersion along the (π,0)-(π,π) cut (Fig. 2C) shows a characteristic kink or break near the Fermi vector (k_F) around 50 meV. This is seen in the original ARPES spectra (Fig. 2A) where an additional narrow peak (denoted by triangle) appears around 50 meV when the broad dispersive peak reaches 100 to 150 meV from the higher binding energy. The narrow peak near E_F is found to disperse more weakly than the broad peak, producing the kink in the energy dispersion. This narrow peak is assigned as a quasiparticle peak produced by the many-body interaction, analogous to that in BSCCO (*22–24*). Comparing the ARPES spectra of the (π,0)-(π,π) cut between NCCO and BSCCO (*25*), we find that the momentum area where the quasiparticle peak appears is much narrower in NCCO than in BSCCO. This may be due to the difference in the energy position of the van Hove singularity at the (π,0) point, which is less than 30 meV from E_F for optimally doped BSCCO and about 350 meV for NCCO.

In the (0,0)-(π,π) cut (Fig. 2, B and D), the ARPES spectral behavior is very different from that of the (π,0)-(π,π) cut. First, the total spectral intensity gradually decreases as the peak approaches E_F in contrast with the gradual increase in the (π,0)-(π,π) cut. Second, a kink in the energy dispersion near k_F is not clearly observed in the (0,0)-(π,π) cut. The gradual suppression in the spectral intensity may be due to a matrix-element effect. The absence of a kink in the energy dispersion in the (0,0)-(π,π) cut corresponds to the absence of a two-peaked structure near E_F in the ARPES spectra (Fig. 2B). The present ARPES result thus shows an anisotropic nature of the many-body interaction in NCCO like that found in BSCCO. However, it is worthwhile to note that despite the similarity in the anisotropic nature of the many-body interaction, there is a qualitative difference in the dispersive feature in the (0,0)-(π,π) cut. The energy dispersion of BSCCO shows a kink structure even along the (0,0)-(π,π) cut (*22–24*), though it is not clearly seen in NCCO. The reason for this difference is not clear at present. We speculate that the many-body interaction, reflected in the difference in the T_c (~90 K in BSCCO and 22 K in NCCO), may be weaker in NCCO than in BSCCO, leading to a weak kink structure in the energy dispersion. The gradual decrease in the spectral intensity toward E_F may conceal the weak kink structure near E_F. The reason for this difference should be elucidated by a higher energy resolved photon-energy dependent ARPES.

In order to see directly the gap-opening behavior, we measured the ultrahigh-resolution ARPES spectra in the vicinity of E_F. ARPES spectra near E_F at 10 K are shown for the two different k_F points, compared with that of gold measured under the same condition (Fig. 3). The leading edge of ARPES spectrum of NCCO at the (π,0)-(π,π) crossing is shifted as a whole toward the high

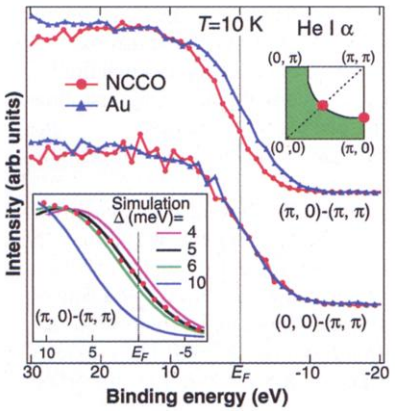

Fig. 3. Angle-resolved photoemission spectra near E_F of $Nd_{2-x}Ce_xCuO_4$ ($x = 0.15$, $T_c = 22$ K) measured at 10 K at the $(\pi,0)$-(π,π) and the (0,0)-(π,π) crossing, compared with the gold reference measured under the same condition. Inset shows the result of numerical fitting with various gap values.

binding energy relative to that of the gold spectrum, indicating that a superconducting gap opens in this direction. In contrast, the leading edge of ARPES spectrum at the (0,0)-(π,π) crossing almost coincides with the gold reference, suggesting no superconducting gap or a very small one. These spectral behaviors are qualitatively the same as those of BSCCO (*12*, *13*), which have established an anisotropic superconducting gap in the hole-doped HTSC. Thus, the present ultrahigh-resolution ARPES clearly shows that an anisotropic superconducting gap opens also in the electron-doped HTSC. Although a possibility of an anisotropic *s* symmetry with a very small gap at the (0,0)-(π,π) crossing is not excluded because of the finite energy resolution, we conclude that the most probable symmetry deduced from the present result is $d_{x^2-y^2}$ as in the hole-doped HTSCs (*12*, *13*).

We now discuss the size of superconducting gap (Δ) in NCCO. The shift of the leading edge of ARPES spectrum at the $(\pi,0)$-(π,π) crossing is about 2 to 3 meV, but it is noted that this value is not equal to the Δ itself because of the finite energy resolution and the thermal broadening. According to the ARPES result on BSSCO (*26*), the gap size is found to be almost twice that of the leading-edge shift. When applied to the NCCO case, we obtain a gap value of 4 to 6 meV. In order to estimate the gap size more quantitatively, we fitted the spectrum by the BCS (Bardeen-Cooper-Schrieffer) spectral function with broadening of 0.1 meV, multiplied by the Fermi-Dirac function and convoluted with the energy resolution, as has been employed in the hole-doped HTSCs (*26*). We found that the leading edge of ARPES spectrum is relatively well fitted, whereas the higher binding-energy part is not so satisfactorily reproduced. This may be due to the incoherent part of the spectral function and the inelastically scattered secondary electrons, which are not accounted in the simulation. The inset to Fig. 3 shows the result of simulation near E_F. The simulation curve with a 10-meV gap, which corresponds to $2\Delta/k_BT_c \sim 10$ as in the optimally doped BSCCO (*26*–*28*), does not fit the experimental result. This suggests that the superconducting gap of NCCO is much smaller than 10 meV, and, as a result, the $2\Delta/k_BT_c$ value is also smaller than that of BSCCO. Simulations with $\Delta = 5 \pm 1$ meV fit the experimental curve relatively well. This result seems consistent with the tunneling experiments that have proposed the Δ being about 4 meV (*2*, *6*, *9*). The $2\Delta/k_BT_c$ value of NCCO is thus nearly half that (8-10) of optimally doped BSCCO (*26*–*28*), but both have the $d_{x^2-y^2}$–like superconducting order parameter. Although this difference may be related to the difference in the details of the electronic structure near E_F such as the position of the van Hove singularity, we leave this as a challenge for theory.

References and Notes

1. R. D. Parks, *Superconductivity* (Dekker, New York, 1969).
2. Q. Huang *et al.*, *Nature* **347**, 369 (1990).
3. D. H. Wu *et al.*, *Phys. Rev. Lett.* **72**, 85 (1993).
4. A. Andreone *et al.*, *Phys. Rev. B* **49**, 6392 (1996).
5. Y. Tokura, H. Takagi, S. Uchida, *Nature* **337**, 345 (1989).
6. F. Hayashi, E. Ueda, M. Sato, K. Kurahashi, K. Yamada, *J. Phys. Soc. Jpn.* **67**, 3234 (1998).
7. C. C. Tsuei, J. R. Kirtley, *Phys. Rev. Lett.* **85**, 185 (2000).
8. J. D. Kokales *et al.*, *Phys. Rev. Lett.* **85**, 3696 (2000).
9. R. Prozorov, R. W. Giannetta, P. Fournier, R. L. Greene, *Phys. Rev. Lett.* **85**, 3700 (2000).
10. L. Alff *et al.*, *Phys. Rev. Lett.* **83**, 2644 (1999).
11. S. Kashiwaya *et al.*, *Phys. Rev. B* **57**, 8680 (1998).
12. Z.-X. Shen *et al.*, *Phys. Rev. Lett.* **70**, 1553 (1993).
13. H. Ding *et al.*, *Phys. Rev. B* **54**, R9678 (1996).
14. After the completion of this work, we became aware of ARPES work by N. P. Armitage *et al.* [e-Print available at http://xxx.lanl.gov/abs/cond-mat/0012003], which comes to essentially the same conclusion.
15. Because the surface degradation was remarkably enhanced at higher temperatures, we could not obtain reliable data at higher temperatures.
16. Y. Sakisaka *et al.*, *Phys. Rev. B* **42**, 4189 (1990).
17. O. Gunnarsson, O. Jepsen, Z.-X. Shen, *Phys. Rev. B* **42**, 8707 (1990).
18. R. O. Anderson *et al.*, *Phys. Rev. Lett.* **70**, 3163 (1993).
19. H. M. Fretwell *et al.*, *Phys. Rev. Lett.* **84**, 4449 (2000).
20. S. V. Borisenko *et al.*, *Phys. Rev. Lett* **84**, 4453 (2000).
21. D. M. King *et al.*, *Phys. Rev. Lett.* **73**, 3298 (1994).
22. T. Valla *et al.*, *Science* **285**, 2110 (1999).
23. A. Kaminski *et al.*, *Phys. Rev. Lett.* **84**, 1788 (2000).
24. P. V. Bogdanov *et al.*, *Phys. Rev. Lett.* **85**, 2583 (2000).
25. M. R. Norman *et al.*, *Phys. Rev. Lett.* **79**, 3506 (1997).
26. H. Ding *et al.*, *Phys. Rev. Lett.* **74**, 2784 (1995).
27. A. V. Fedorov *et al.*, *Phys. Rev. Lett.* **82**, 2179 (1999).
28. J. Mesot *et al.*, *Phys. Rev. Lett.* **83**, 840 (1999).
29. M. R. Norman *et al.*, *Nature* **392**, 157 (1998).

30. Supported by grants from the CREST (Core Research for Evolutional Science and Technology) Corporation of JST, the Japan Society for Promotion of Science (JSPS), and the Ministry of Education, Science and Culture of Japan. T.S. thanks the JSPS for financial support.

5 December 2000; accepted 13 January 2001

Rapid Electron Tunneling Through Oligophenylenevinylene Bridges

Hadley D. Sikes,[1] John F. Smalley,[2]* Stephen P. Dudek,[1] Andrew R. Cook,[2] Marshall D. Newton,[2]* Christopher E. D. Chidsey,[1]* Stephen W. Feldberg[2]*

We measured rate constants of thermal, interfacial electron transfer through oligophenylenevinylene bridges between a gold electrode and a tethered redox species in contact with an aqueous electrolyte using the indirect laser-induced temperature jump technique. Analysis of the distance dependence indicates that, unlike other bridges studied to date, the rate constants are not limited by electronic coupling for bridges up to 28 angstroms long. The energy levels of the bridges relative to those of the redox species rule out hopping through the bridge. We conclude that, out to 28 angstroms, the transfer is limited by structural reorganization and that electron tunneling occurs in less than 20 picoseconds, suggesting that oligophenylenevinylene bridges could be useful for wiring molecular electronic elements.

The development of novel electronic devices based on molecular materials such as organic light-emitting diodes (*1*, *2*), biosensors (*3*), and molecular electronic devices (*4*) is focusing interest on electron transfer across interfaces between conventional electrodes and molecular materials and, specifically, on the promotion of fast electron transfer through molecular bridges over large distances. The distance dependences of rate constants reported thus far for long-distance electron-transfer reactions involving a single electron tunneling step are well described by the superexchange model (*5*, *6*) in which the elec-